ENGINEERING TRANSACTIONS • *Engng. Trans.* • **48**, 3, 329–340, 2000
Polish Academy of Sciences • Institute of Fundamental Technological Research
10.24423/engtrans.596.2000

ON INFLUENCE OF PAD FEATURES ON DYNAMICS OF A RAILWAY TRACK

R. BOGACZ ([1,2]), A. KAMIŃSKI ([3]), T. KRZYŻYŃSKI ([1,4])

([1]) **POLISH ACADEMY OF SCIENCES**
INSTITUTE OF FUNDAMENTAL TECHNOLOGICAL RESEARCH
Świętokrzyska 21, 00–049 Warszawa, Poland

([2]) **WARSAW UNIVERSITY OF TECHNOLOGY**

([3]) **PKP (POLISH RAILWAY COMPANY)**

([4]) **TECHNICAL UNIVERSITY OF KOSZALIN**

The vertical track dynamic model is described in the paper as a periodic structure. It is composed of rails modelled as Timoshenko or Bernoulli-Euler beams, sleepers (lumped masses) and pads and ballast modelled as viscoelastic elements. Particular attention is paid to the influence of pad characteristics on the dynamic stiffness of the track. One of the ideas of the new pad generation is also presented in the paper. Some parameters of the pad are given.

1. INTRODUCTION

The conventional railway track is composed of two rails mounted on the sleepers by means of pads. In this paper the case of free wave propagation is investigated. In the system under consideration, a single rail is modelled as a Timoshenko beam. The rails are coupled by means of periodically spaced sleepers which are modelled as lumped bodies with one or two degrees of freedom, i.e. vertical displacement and rotation. Dynamical analysis of the railway track as a typical periodic system bases on Floquet's theorem and makes it possible to study the influence of the pad feature on the track dynamics.

2. Formulation of the problem

The system under consideration consists of two parallel infinite subsystems (rails), Fig. 1, which are coupled by means of equally spaced sleepers. Assuming longitudinal symmetry of the track we model the rails as two Timoshenko beams of the same parameters. The equations of motion of the Timoshenko beam resting on a viscoelastic foundation, which is subjected to the load $p(x,t)$, are taken in the following form:

$$K\frac{\partial}{\partial x}\left(\frac{\partial w}{\partial x}-\varphi\right)-\rho A\frac{\partial^2 w}{\partial t^2}-\eta\frac{\partial w}{\partial t}-qw+p(x,t)=0,$$

(2.1)

$$EI\frac{\partial^2\varphi}{\partial x^2}+K\left(\frac{\partial w}{\partial x}-\varphi\right)-\rho I\frac{\partial^2\varphi}{\partial t^2}=0,$$

where: $w=w(x,t)$ is the displacement, $\varphi=\varphi(x,t)$ is the rotation of a beam cross-section due to the bending moment, both of them being functions of the special variable x and time t. In Eqs. (2.1) $K=\kappa GA$ denotes the shear stiffness, EI is the flexural rigidity, ρA is the beam mass per unit length, ρI is the rotatory inertia of a beam cross-section, q and η denote the coefficients of elasticity and damping of the foundation, respectively. The periodicity of the railway track, Fig. 1, results in the following boundary conditions for the functions w and φ:

$$w(nl_-,t)=w(nl_+,t),\quad \varphi(nl_-,t)=\varphi(nl_+,t), \tag{2.2}$$

$$-EI\frac{\partial\varphi}{\partial x}(nl_-,t)+EI\frac{\partial\varphi}{\partial x}(nl_+,t)=0, \tag{2.3}$$

$$-K\left[\frac{\partial w}{\partial x}(nl_-,t)-\varphi(nl_-,t)\right]+K\left[\frac{\partial w}{\partial x}(nl_+,t)-\varphi(nl_+,t)\right]-R(nl,t)=0, \tag{2.4}$$

where l is the spacing of the sleepers, n is the support number ($n\in\{-\infty,...,-1,0,1,...,+\infty\}$). Eqs. (2.2) – (2.4) represent the continuity of the displacement, rotation, bending moment and the equilibrium of shearing forces, respectively, for the n-th periodic support. The sleeper-rail interaction force $R=R(nl,t)$ can be determined by means of the consideration concerning the dynamics of sleepers.

The sleeper is modelled as a rigid body with two degrees of freedom (vertical displacement and rotation) resting on a viscoelastic foundation, which is mounted on the rails by means of the pads modelled as viscoelastic elements. The equations of motion of the n-th sleeper read

$$R=R(nl,t)=q_P(w-u)+\eta_P\left(\frac{dw}{dt}-\frac{du}{dt}\right), \tag{2.5}$$

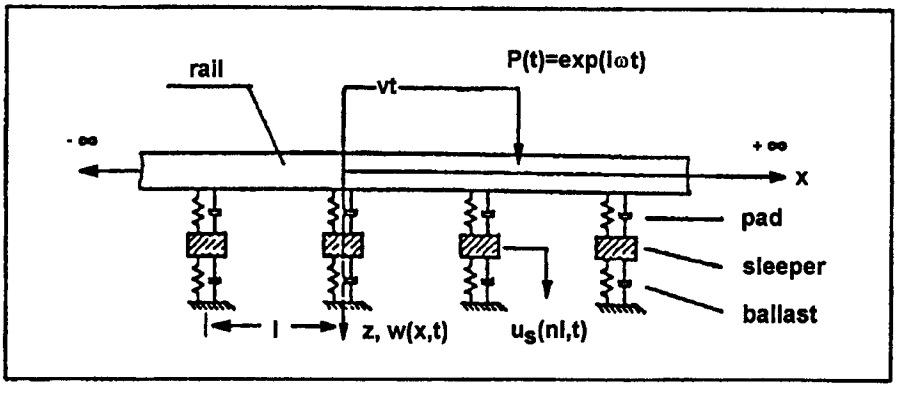

FIG. 1. Model of one infinite subsystem.

where $u = u(nl, t)$ denotes the displacement of the n-th sleeper at the mounting point, R is the force of the pad. The displacement $u = u(nl, t)$ is described by the following equation:

$$m_S \frac{d^2u}{dt^2} + \eta \frac{du}{dt} + qu = R, \tag{2.6}$$

with the notation:

$m_S = \mu_S l_S$	$q = q_B l_S$	$\eta = \eta_B l_S$
l_S – sleeper length μ_S – sleeper mass per unit length q_B – ballast elasticity coefficient per length η_B – ballast damping coefficient per length q_P – pad elasticity coefficient η_P – pad damping coefficient		

For the steady-state motion with the frequency ω, the interaction force $R = R(nL, \tau)$ determined for the n-th sleeper reads

$$\begin{aligned} R(nl,t) &= (q_P + i\eta_P\omega)[w(nl,t) - u(nl,t)], \\ R(nl,\omega) &= \Delta(\omega) w(nl,\omega), \end{aligned} \tag{2.7}$$

where

$$\begin{aligned} \Delta(\omega) &= \frac{(q_P + i\omega\eta_P)(-\omega^2 m_S + q + i\omega\eta)}{-\omega^2 m_S + q + q_P + i\omega(\eta_P + \eta)}, \\ R(nl,\omega) &= (-m_S\omega^2 + \eta i\omega + q)u. \end{aligned}$$

For the analysis which follows we introduce the non-dimensional quantities which are given in the table below.

The non-dimensional form of the equations of motion, Eqs. (2.1), reads

$$\frac{1}{\alpha}\frac{\partial}{\partial X}\left(\frac{\partial W}{\partial X}-\psi\right)-\frac{\partial^2 W}{\partial \tau^2}-N\frac{\partial W}{\partial \tau}-QW+P(X,\tau)=0,$$

(2.8)

$$\frac{\partial^2 \psi}{\partial X^2}+\frac{1}{\alpha}\left(\frac{\partial W}{\partial X}-\psi\right)-\beta\frac{\partial^2 \psi}{\partial \tau^2}=0.$$

The boundary conditions given by Eqs. (2.2) – (2.4) take now the following form:

(2.9) $$W(nL_-,\tau)=W(nL_+,\tau),\quad \psi(nL_-,\tau)=\psi(nL_+,\tau),$$

(2.10) $$-\frac{\partial \psi}{\partial X}(nL_-,\tau)+\frac{\partial \psi}{\partial X}(nL_+,\tau)=0,$$

(2.11) $$-\frac{1}{\alpha}\left(\frac{\partial W}{\partial X}-\psi\right)_{nL_-}+\frac{1}{\alpha}\left(\frac{\partial W}{\partial X}-\psi\right)_{nL_+}-\tilde{R}(nL,\tau)=0,$$

where

(2.12) $$\tilde{R}(n,L)=\frac{a_0}{E}\Delta(\omega).$$

The rail parameters are:

$X=xa_0$	$\tau=t\omega_0$	$W(X,\tau)=w/w_0$
$\psi=\varphi/(a_0\omega_0)$	$\Omega=\omega/\omega_0$	$V=v/v_0$
$N=\eta/\eta_0$	$Q=q/E$	$\alpha=\rho/Kv_0^2$
$\beta=\rho/Ev_0^2$	$K=\kappa AG$	$L=l/a_0$
$\eta_0=\sqrt{E\mu}$	$a_0=\sqrt[4]{1/I}$	$\omega_0=\sqrt{E/\mu}$
$w_0=p_0a_0/E$	$v_0=\omega_0/a_0$	

In the next part of the paper we find the solution of Eqs. (2.8) with the conditions (2.9), (2.10) and (2.11) in the case of free wave propagation.

3. Travelling wave propagation in a railway track

The solutions in the case of free wave propagation ($P(X,\tau)=0$) can be written in the following form:

$$W(X,\tau) = A_w(X\lambda)\cdot\exp[i(\lambda X+\Omega\tau)],$$

(3.1)

$$\psi(X,\tau) = A_\psi(X,\lambda)\cdot\exp[i(\lambda X+\Omega\tau)].$$

We assume that the functions $A_w = A_w(X,\lambda)$, $A_\psi = A_\psi(X,\lambda)$ describe dynamically admissible displacement fields. According to Floquet's theorem we suppose they are periodic functions, i.e. functions which are independent of the choice of a cell of the periodic structure, $A_w(X+L\lambda) = A_w(X,\lambda)$, $A_\psi(X+L\lambda) = A_\psi = (X,\lambda)$. Introduction of the relations (3.1) into Eqs. (2.8), in which we put $P(X,\tau) = 0$, yields the following set of equations:

$$\frac{1}{\alpha} D_A(D_A A_w - A_\psi) + \Omega^2 A_w - iN\Omega A_w - QA_w = 0,$$

(3.2)

$$D_A^2 A_\psi + \frac{1}{\alpha}(D_A A_w - A_\psi) + \beta\Omega^2 A_\psi = 0.$$

The differential operator D_A reads

$$D_A = D_A(X,\lambda) = i\lambda + \frac{d}{dX}. \tag{3.3}$$

The conditions for the functions $A_w = A_w(X,\lambda)$, $A_\psi(X,\lambda)$, which follow from the boundary conditions given by Eqs. (2.10) and (2.11), read

$$A_w[(n+1)L] = A_w(nL), \quad A_\psi[(n+1)L] = A_\psi(nL), \tag{3.4}$$

$$-D_A A_\psi[(n+1)L] + D_A A_\psi(nL) = 0, \tag{3.5}$$

$$(D_A^2 + \beta\Omega^2)A_\psi[(n+1)L] - (D_A^2 + \beta\Omega^2)A_\psi(nL) + \Delta(\Omega)A_w(nL) = 0. \tag{3.6}$$

The solution of Eqs. (3.2) can be written in the form

$$A_w = \sum_{m=1}^{4} a_{w_m} e^{a_m X}, \quad A_\psi = \sum_{m=1}^{4} a_{\psi_m} e^{a_m X}. \tag{3.7}$$

In Eqs. (3.7) we have

$$\begin{aligned} &\alpha_{1,2} = -i(\lambda \mp s_1), && \alpha_{3,4} = -i(\lambda \mp s_2), \\ &s_1 = \sqrt{(-b_s - \sqrt{b_s^2 - 4c_s})/2}, && s_2 = \sqrt{(-b_s + \sqrt{b_s^2 - 4c_s})/2}, \\ &b_s = -\Omega^2(\alpha+\beta) + \alpha(Q + iN\Omega), && c_s = (Q + iN\Omega - \Omega^2)(1 - \alpha\beta\Omega^2). \end{aligned} \tag{3.8}$$

Introduction of Eqs. (3.7) into the boundary conditions given by Eqs. (3.4) – (3.6) yields A_w and A_ψ. In the case of a beam described by the Bernoulli-Euler beam theory, the displacement is given by the following expression:

$$W(X,\tau) = A_w(\xi,\lambda)\,\exp[i(\lambda nL + \Omega\tau)], \tag{3.9}$$

where

$$A_w(\xi,\lambda) = [\sin S\xi e^{i\lambda L} + \sin S(L-\xi)](\cos\lambda L - \cos SL) + \tag{3.10}$$
$$-[\sin\mathrm{h}S\xi e^{i\lambda L} + \sin\mathrm{h}S(L-\xi)](\cos\lambda L - \cos SL),$$

in the case when

$$X \in \langle n_1 L, n_2 L\rangle, \quad \xi = X - n_1 L, \quad \xi \in \langle 0, L\rangle, \quad S^2 = \sqrt{\Omega^2 - iN\Omega - Q}.$$

Eq. (3.9) describes a travelling wave in periodic structure of the shape given by function (3.10). The dispersion relation between frequency Ω and wave number λ is given by the following equation:

$$f(\lambda,\Omega) = \cos^2\lambda L - \cos\lambda L\,[\cos SL + \cos\mathrm{h}SL \tag{3.11}$$
$$+\frac{\Delta(\Omega)}{4S^3}(\sin SL - \sin\mathrm{h}SL)\Big] + \cos SL\cos\mathrm{h}SL$$
$$+\frac{\Delta(\Omega)}{4S^3}(\sin SL\cos\mathrm{h}SL - \sin\mathrm{h}SL\cos SL) = 0.$$

In the general viscoelastic case the dispersion relation (3.11) is satisfied by a complex wave number $\lambda = \lambda_R + i\lambda_1$, with the wave number $\lambda_R = \mathrm{Re}(\lambda)$ and the attenuation number $\lambda_1 = \mathrm{Im}(\lambda)$. The solution given by Eq. (3.9) takes the form

$$W(X,\tau) = \overline{A}_w(\xi,\lambda)\cdot\exp\{-\lambda_1 nL + i[(\lambda_R nL + \Omega\tau)]\}, \tag{3.12}$$

with

$$\overline{A}_w(\xi,\lambda) = A_w(X,\lambda)\exp(i\xi\lambda). \tag{3.13}$$

In a purely elastic case ($\eta = 0$, $\eta_P = 0, \eta_B = 0$, $\Delta(\Omega) = \mathrm{const}$) one can distinguish two characteristic cases. For $\lambda_I = 0$, $\lambda_R \neq 0$, travelling waves given by Eq. (3.12) propagate in the whole infinite structure, which corresponds to the so-called 'passing bands' in the (Ω,λ)-plane, (BRILLOUIN [2]). For $\lambda_I \neq 0$, the waves cannot propagate and their attenuation in space is determined by the term $\exp(-\lambda_I nL)$, which corresponds to 'stopping bands' in the (Ω,λ)-plane.

Numerical calculations have been carried out for the Bernoulli-Euler beam ($\alpha = 0$, $\beta = 0$) (BOGACZ *et al.* [1]), and for the system parameters presented in Table 1. The first Brillouin zone (or propagation zone), (BRILLOUIN [2]), (MEAD [5]) for $l = 0.6$ m reads $\lambda_R \in \langle -\pi/l, \pi/l\rangle = \langle -5.24\ \mathrm{rad/m},\ 5.24\ \mathrm{rad/m}\rangle$.

The case shown in Fig. 2 illustrates the displacement of rails and sleepers for given frequencies and time 0, $\frac{1}{8}T$, $\frac{1}{4}T$, and $\frac{3}{8}T$, respectively.

Table 1. System parameters, the Bernoulli-Euler beam ($\alpha = 0, \beta = 0$).

$E = 2.1\ 10^{11}\ \frac{N}{m^2}$	$I = 3.052\ 10^{-5} m^4$	$\mu = 60.31\ \frac{kg}{m}$
$\eta = 4\ 10^4 \frac{N_S}{m^2}$	$l_S = 2.36$ m	$l_P = 1.435$ m
$q_P = 2.6\ 10^8\ \frac{N}{m}$	$\eta_P = 6.3\ 10^4\ \frac{N_S}{m}$	$\mu_S = 122.88\ \frac{kg}{m}$
$q_B = 1.525\ 10^8\ \frac{N}{m^2}$	$\eta_B = 6.95\ 10^4\ \frac{N_S}{m^2}$	$l = 0.6$ m

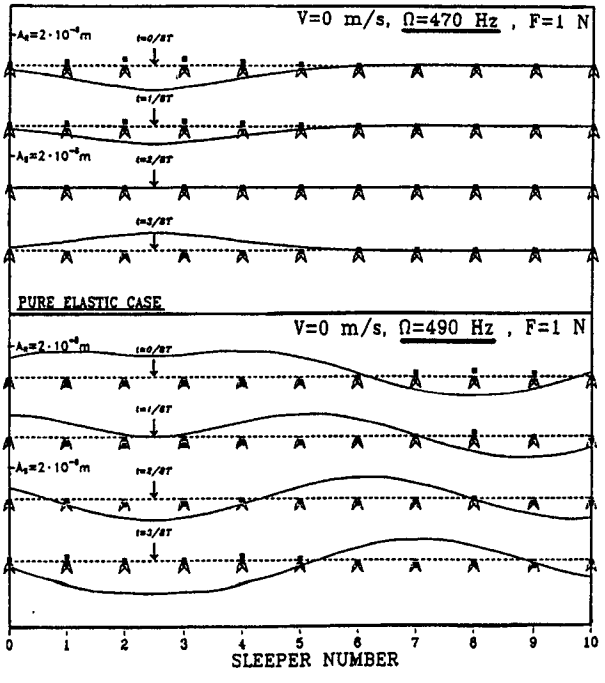

FIG. 2. Displacement of rails and sleepers for given frequency and time 0, $\frac{1}{8}T$ and $\frac{3}{8}T$.

The stopping and passing bands in the frequency ranges are presented in Table 2.

Table 2. Configuration of the bands [Hz], ($\alpha = 0, \beta = 0$).

Passing bands	(156.2, 263.9)	(481.4, 1422.4)	(1547.1, 5690.0)
Stopping bands	(0, 156.2)	(263.9, 481.4)	1422.4, 1547.1)

For a frequency equal to 277.0 Hz, which is an in-phase eigenfrequency of the system pad-sleeper-ballast, the contrast force in a pad tends to infinity and the

flexible supports become rigid ones what results in a decoupling of the adjacent cells of the periodic system (Table 3).

Table 3. Selected system of eigenfrequencies and corresponding eigenforms, ($\alpha = 0, \beta = 0$).

Frequency [Hz]	Phase relation of a sleeper and a rail point above it	Phase relation of rail points above adjacent sleepers
156.2(**154.4**)	in-phase	in-phase
263.9(**271.7**)	in-phase	out-of-phase
481.4(**487.0**)	out-of-phase	in-phase
1547.1(**1547.3**)	out-of-phase	out-of-phase

In the frequency range (277.0, 481.4) Hz we have the so-called 'propagating and attenuating waves'. The frequency 1422.4 Hz is the eigenfrequency of a simply supported beam of the same length and the same other parameters as the periodic cell. The corresponding eigenform is the so-called 'pinned-pinned' mode, (KRZYŻYŃSKI [4]), with nodes at the periodic supports. The dispersion relations (3.11) calculated for the elastic and viscoelastic case are given in the above quoted paper. The dynamic stiffness for the case of small and large damping (dashed line) is illustrated in Fig. 3.

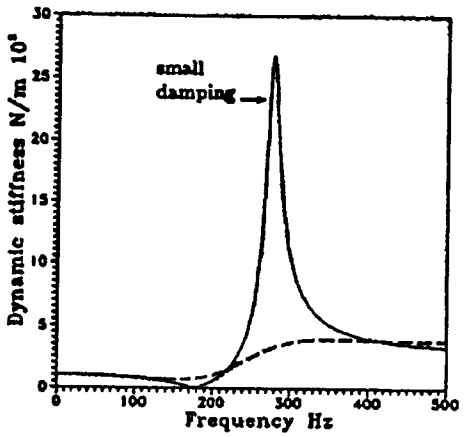

FIG. 3. Dynamic stiffness for almost elastic and viscoelastic case (dashed line).

As we can see, very high growth of dynamic stiffness may occur in relatively small range of frequency.

The influence of the pad elasticity q_p on the dynamic stiffness of the rail-sleeper-ballast system is illustrated in Fig. 4. The curve No. 1 represents the

system described by parameters given in Table 1. The curve No. 2 is obtained for two times greater value of the nominal q_p, i.e. ($q_p = 5.2 \cdot 10^8$ N/m). The curve No. 3 represents value of $q_p = 1.04 \cdot 10^9$ N/m and the curve No. 4 corresponds to $q_p = 2.08 \cdot 10^9$ N/m.

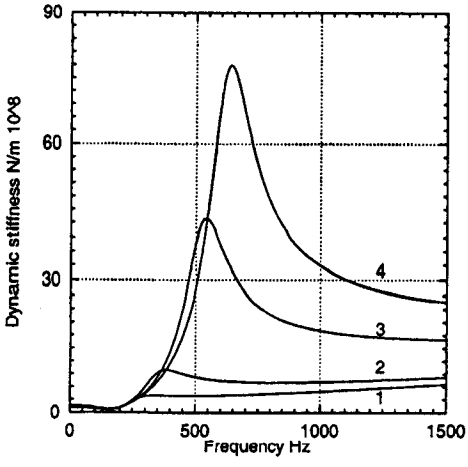

FIG. 4. Dynamic stiffness versus frequency for chosen values of pad elasticity.

As follows from the curves presented on the graphs, the dynamic stiffness versus parameter of pad elasticity has a progressive characteristic. Also the frequency and its range is growing with pad stiffness.

The results of the above investigations show that the choice of viscoelastic parameters of the pad can be very important for proper wheel/rail system interaction. The characteristic of the rail/sleeper interaction depends on such parameters as: temperature, frequency, humidity, time in service and other.

The dependence of the number of cycles of loading in the case of a new generation of the pad used by Polish Railway and PANDROL company and tested on the set shown in Fig. 5, is illustrated in Fig. 6.

We can state that the static displacement is systematically growing but the change of stiffness is negligible. The influence of temperature on the pad dynamic characteristics for two kinds of pads at temperature $+20°$ C and $-25°$ C is shown in Fig. 7. Dashed line shows the UIC-864-5 standard edited by Kamiński, and the continuous line describes this dependence for the new shape of pad.

One can notice that the stiffness of the UIC pad is much higher than the new one and has greater influence on the temperature lowering, while the disadvantage of the new pad is the increase in deflection difference at load limits. The change of characteristics for the case of the standard German pad (type Zw 700) at the temperature between $+50°$ C and $-30°$ C is rather large, what is shown in Fig. 8.

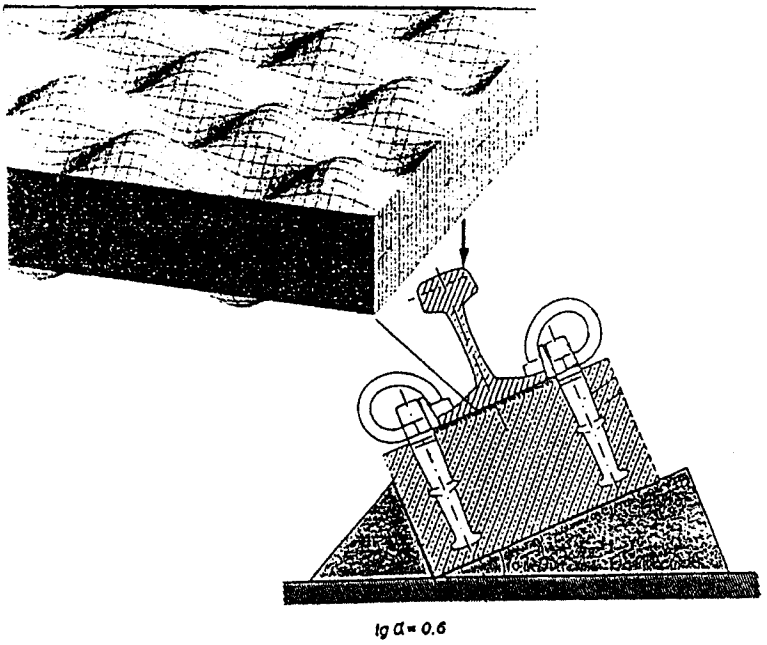

FIG. 5. The pad of new generation (PKW60K1) and shema of the stand for investigation of pads under cycling loading.

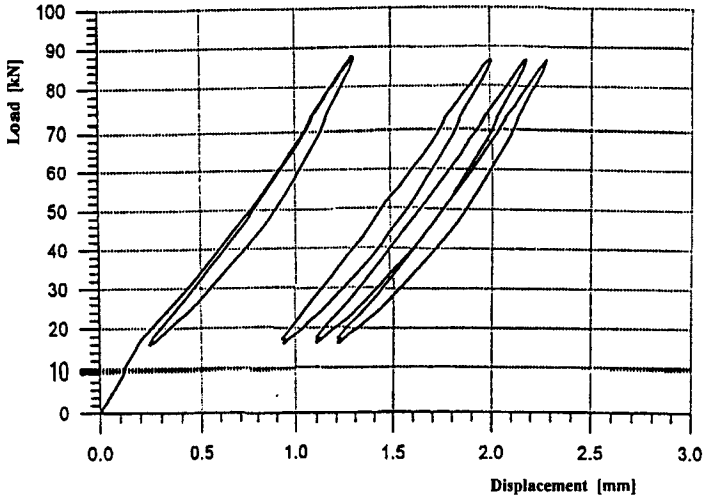

FIG. 6. The force versus displacement for loops at frequency 10 Hz for 1st, 200000, 600000, and 1000000 cycles, respectively.

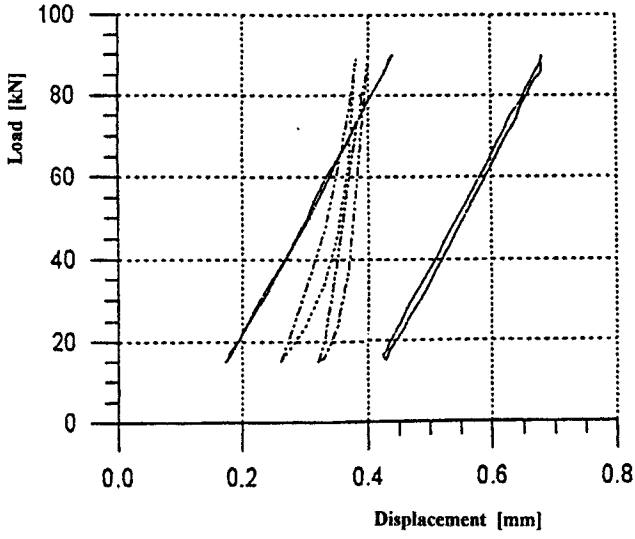

FIG. 7. Force-displacement relations for two kinds of pads, dashed line denotes UIC. Standard, continuous line – new pad.

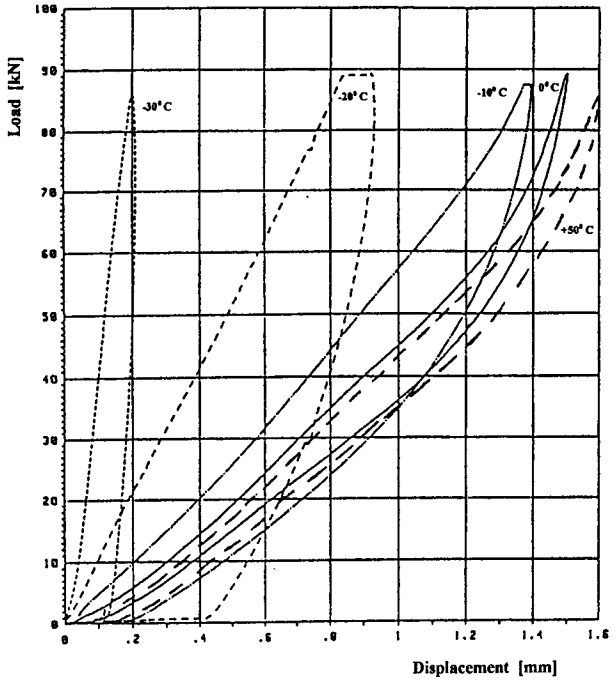

FIG. 8. The force-displacement characteristics for the pad ZW 700 at the temperature $-30°$ C, $-20°$ C, $-10°$ C, $0°$ C and $+50°$ C, respectively.

4. Conclusions

The method applied in the paper consists in the direct application of Floquet's theorem to differential equations of motion of the beam. Arranging the periodic boundary conditions for the whole infinite system makes it possible to reduce the analysis to one cell of the periodic structure. There are two forms of travelling wave propagation in the case of an unloaded periodic structure.

As follows from the investigations, the very high increase in the dynamic stiffness of the pad occurs in the case of relatively stiff pads. This is the reason why the initiation of the corrugation takes place in the areas located over the sleepers. We hope that further optimisation of the pad features will enable better conditions of wheel/rail interaction.

The analysis of dynamic pad stiffness, which takes into account the influence of ballast and subgrade dynamics proposed in this paper, has been carried out for a relatively simple track model. This approach can be easily extended and applied to more complex models which will be the subject of the author's further publications.

References

1. R. Bogacz, T. Krzyżyński and K. Popp, *Influence of shear deformation and rotatory inertia on the solutions of the generalized Mathew's problem*, Z. Angew. Math. Mech., **73**, 1, 5–13, 1993.
2. L. Brillouin, *Wave propagation in periodic structures*, Dover Publications, 1953.
3. A. Kamiński, ERRI Report on Measurements Parts of Track, Utrecht, May, 1995.
4. T. Krzyżyński, *On continuous subsystem modelling in the dynamic interaction problem of a train-track system*, Suppl. Vehicle System Dynamics, **24**, 311–324, 1995.
5. D. J. Mead, *A new method of analyzing wave propagation in periodic structures*, J. Sound Vibr., **104**, 1, 9–27, 1986.

Received April 17, 2000.